Steel and Composite Structures, *Vol. 21, No. 5 (2016) 1121-1144*
DOI: http://dx.doi.org/10.12989/scs.2016.21.5.1121

Advanced analysis for planar steel frames with semi-rigid connections using plastic-zone method

Phu-Cuong Nguyen [a] and Seung-Eock Kim [*]

Department of Civil and Environmental Engineering, Sejong University, 98 Gunja-dong, Gwangjin-gu, Seoul 143-747, South Korea

(*Received January 04, 2016, Revised June 22, 2016, Accepted July 26, 2016*)

Abstract. This paper presents a displacement-based finite element procedure for second-order distributed plasticity analysis of planar steel frames with semi-rigid beam-to-column connections under static loadings. A partially strain-hardening elastic-plastic beam-column element, which directly takes into account geometric nonlinearity, gradual yielding of material, and flexibility of semi-rigid connections, is proposed. The second-order effects and distributed plasticity are considered by dividing the member into several sub-elements and meshing the cross-section into several fibers. A new nonlinear solution procedure based on the combination of the Newton-Raphson equilibrium iterative algorithm and the constant work method for adjusting the incremental load factor is proposed for solving nonlinear equilibrium equations. The nonlinear inelastic behavior predicted by the proposed program compares well with previous studies. Coupling effects of three primary sources of nonlinearity, geometric imperfections, and residual stress are investigated and discussed in this paper.

Keywords: distributed plasticity; nonlinear inelastic analysis; second-order effects; semi-rigid connections; steel frames

1. Introduction

Practical analysis and design software programs for framed structures such as STAAD Pro, SAP2000, MIDAS, etc., often adopt the plastic hinge method for framed members to analyze the structure because of its simplicity and acceptable accuracy. Hoang *et al*. (2015) reviewed the plastic hinge analysis of 3D steel frames. However, in some specific cases, the plastic hinge method overestimates the ultimate load and strength of the structure (King *et al*. 1992, White 1993, White and Chen 1993), which can lead to unsafe designs. Moreover, if members gradually yield along their length due to mainly the axial force, the plastic hinge model is not suitable more. One method which analyzes more accurately and consumes a lot of source of computer is called the distributed plasticity method (plastic-zone method). This method can "suitably" predict the behavior of the structure and monitor responses of sub-element inside the member. Therefore, with powerful computer technology nowadays, the distributed plasticity method will replace the plastic hinge method in the problems with higher accuracy and in the detail design.

∗Corresponding author, Professor, E-mail: sekim@sejong.ac.kr
[a] Ph.D., E-mail: henycuong@sejong.ac.kr; henycuong@gmail.com

http://www.techno-press.org/?journal=scs&subpage=6 ISSN: 1229-9367 (Print), 1598-6233 (Online)

The distributed plasticity method is based on the finite element method. There are two types of the distributed plasticity method in the literature. The first method type uses shell elements for modeling the beam-column element (Avery and Mahendran 2000, Mahendran and Avery 2000, Kim and Lee 2002). This method can trace the local buckling and warping effects in the member. Although finite element solutions using shell elements are more accurate than those of beam elements, it is complicated and expensive in terms of computer sources and computational time for performing multi-story frames. Therefore, the second method type using beam-column elements is more favorable and common (Attalla *et al*. 1994, Foley and Vinnakota 1997, 1999, Teh and Clarke 1999, Foley 2001, Alemdar and White 2005, Chiorean 2009, Rigobello *et al*. 2013, Nguyen and Kim 2014, Saritas and Koseoglu 2015). In this method, the beam-column member is divided into several sub-elements and each cross-section of the sub-element is divided into many small fibers. Fibers are monitored, and their stress and strain are estimated. Then, geometric characteristics of each section of the sub-element are updated, finally assembling the instantaneous stiffness matrix of the beam-column member.

In the last two decades, there have been several researches using the distributed plasticity method; herein, we summarize some typical studies. Foley and Vinnakota (1997, 1999) proposed a nonlinear finite element procedure for the second-order distributed plasticity analysis of multi-storey planar steel frames under static loadings. The steel stress-strain relationship is assumed to be the elastic-perfectly plastic model. In order to improve computational performance, Foley (2001) proposed parallel processing and vectorization, in which a main structure is separated into several sub-structures for reducing unknowns of system equations. Alemdar and White (2005) presented different procedures based on displacement, flexibility, and mixed beam–column formulations using a total Lagrangian corotational approach for the distributed plasticity analysis of frame structures. In recent years, Chiorean (2009) derived a complicated beam-column method for the second-order inelastic analysis of space steel frames with semi-rigid connections. The advantage of this study was that it is able to trace the distributed plasticity along the member length by using only one beam-column element per frame member in analytical modeling. However, it seems that the shape parameters a and n of the Ramberg-Osgood model and α and p of the proposed modified Albermani model for the force-strain relationship of the cross-section, which consider the effect of the gradual yielding behavior of members, need to be investigated more adequately. Rigobello *et al*. (2013) proposed a solid-like finite element for second-order inelastic analysis of steel frames. They used a multi-fiber beam-column element with an enhanced formulation for considering initially curved elements, warping mode, complete 3D constitutive model, any cross section geometry, arbitrary reference line, geometrically exact description and strain with linear variation along transverse direction. Therefore, they called the developed finite element as “solid-like”, as it considers such aspects achieved only with solid elements. Nguyen and Kim (2014, 2015) presented a second-order distributed plasticity analysis method for steel frames using only one beam-column element per frame member by employing stability functions, in which the elemental axial stiffness and bending stiffness are sensitive to the number of integration points due to the important influence of weight factors (i.e., if plastic hinges only form at two ends of the member, using two integration points gives a smaller stiffness than using ten integration points for a member due to the weight factors being distributed more uniformly for ten monitoring points). Therefore, choosing the number of integration points acts on the final response of structures. Also in this way, the effect of the shift of the elastic core during the yielding processing is difficult to consider exactly. Such proposed formulations can underestimate the load-carrying capacity and performance of frame structures. To obtain a high accuracy, it is necessary that members are

completely divided into a lot of sub-elements along their length. After that, stiffness matrices of sub-elements are assembled to form a stiffness matrix at the member level.

In recent years, Gorgun (2013) and Valipour and Bradford (2013) analyzed the nonlinear behavior of planar steel frames with semi-rigid connections without the effect of material inelasticity. Bandyopadhyay *et al.* (2015) employed the commercial FEM software SAP2000 for analyzing the static inelastic behavior of planar steel frames using the plastic hinge method.

In this study, a second-order distributed plasticity analysis method for planar steel frame with semi-rigid connections is proposed. The material nonlinearity is taken into account by the distributed plasticity method. The behavior of steel material conforms to an elastic-perfectly plastic material model with linear strain hardening. The distributed plasticity is considered by the beam-column finite element method. Initial residual stresses are assigned for every fiber of cross-sections. The second-order effect (the P – small delta effect) is also considered through dividing the member into several sub-elements and forming the elemental finite element formulation. One disadvantage of commercial analysis and design software programs is that semi-rigid connections are simulated as springs with constant stiffness. In reality, the moment-rotation relationship of connections is nonlinear curves with gradual decreasing stiffness. This study employs the Kishi-Chen power model (Chen and Kishi 1989) and the Lui-Chen exponential model (Lui and Chen 1986) for the moment-rotation curve of connections. Verification examples are compared with previous studies to verify accuracy of the proposed procedure. A case study, a 5-storey 4-bay steel frame with semi-rigid connections is investigated. Percentage of yielding of the structure is illustrated. The proposed program can be used to develop a second-order distributed plasticity analysis program for 3D steel frames with semi-rigid connections.

2. Nonlinear finite element formulation

2.1 Beam-column element considering the distributed plasticity and second-order effects

A typical beam-column member subjected to loads is illustrated in Fig. 1. In order to capture the distributed plasticity, the beam-column member is divided into n elements along the member length as illustrated in Fig. 2; each element cross-section is divided into m small fibers as illustrated in Fig. 3; and, each fiber is represented by its material properties, geometric characteristic, area A_j, and its coordinate location (y_j, z_j) corresponding to its centroid. By this way, residual stress is directly considered in assigning an initial stress value for each fiber. The second-order effects are included by the use of several sub-elements per member through updating of the element stiffness matrix and nodal coordinates at each iterative step.

To reduce computational time when assembling the structural stiffness matrix and solving the system of nonlinear equations, n sub-elements are condensed into a typical beam-column member

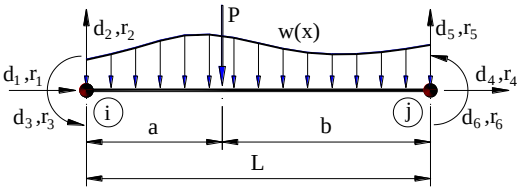

Fig. 1 Beam-column element modeling under arbitrary loads

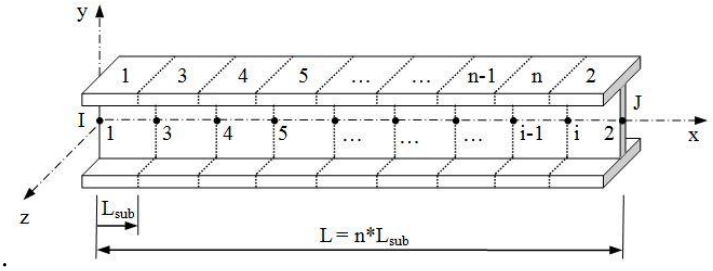

Fig. 2 Meshing of beam-column element into n sub-elements

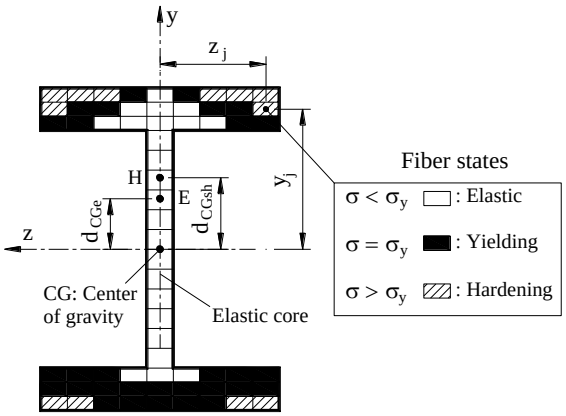

Fig. 3 Illustration of meshing of element cross-section and states of fibers

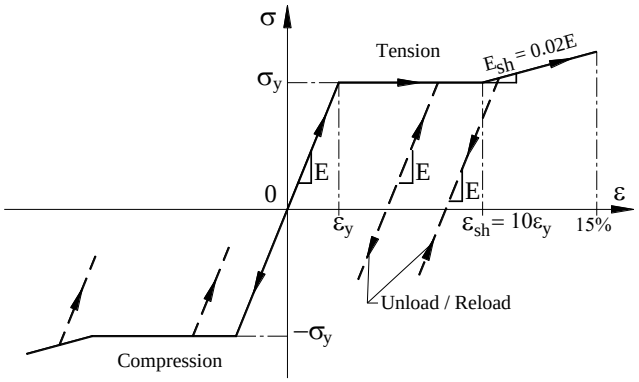

Fig. 4 Constitutive model is assumed for steel material

with the six degrees of freedom at the two ends by using the static condensation algorithm derived by Wilson (1974). The reverse condensation algorithm is used to find the displacements along the member length for evaluating the effects of distributed plasticity and the second-order effects.

In the development of the second-order distributed plasticity beam-column element, the following assumptions are made: (1) the element is initially straight and prismatic; (2) plane cross-sections remain plane after deformation and normal to the deformed axis of the element; (3) out-

of-plane deformations and the effect of Poisson are neglected; (4) shear strains are negligible; (5) member deformations are small, but overall structure displacements may be large; (6) residual stress is uniformly distributed along the member length; (7) yielding of the cross-section is governed by only normal stress; (8) the material model is linearly strain-hardening elastic-perfectly plastic; and, (9) local buckling of the fiber elements does not occur. In this study, an elastic-perfectly plastic stress-strain relationship with linearly strain hardening used by Toma and Chen (1992) is adopted as shown in Fig. 4. Strain hardening starts at the strain of $\varepsilon_{sh} = 10\ \varepsilon_y$, and its modulus E_{sh} is assumed to be equal to 2% of the elastic modulus E. The total internal strain energy of a beam-column element can be expressed as follows

$$U = \int_V \int_\varepsilon \sigma d\varepsilon dV \tag{1}$$

The normal stresses corresponding to the strain state of fibers are calculated as follows

$$\begin{aligned} &\sigma = E\varepsilon && \text{for elastic fibers} \\ &\sigma = E\varepsilon_y = \sigma_y && \text{for yielding fibers} \\ &\sigma = E\varepsilon_y + E_{sh}\left(\varepsilon - \varepsilon_{sh}\right) = \sigma_{sh} && \text{for hardening fibers} \end{aligned} \tag{2}$$

The total internal strain energy of a partially strain-hardening elastic-perfectly plastic beam-column element can be expanded as

$$\begin{aligned} U = &\int_{V_e}\int_0^\varepsilon E\varepsilon d\varepsilon dV_e + \int_{V_p}\left(\int_0^\varepsilon \sigma_y d\varepsilon - \int_0^{\varepsilon_y} E\varepsilon d\varepsilon\right) dV_p \\ &+ \int_{V_{sh}}\left\{\int_0^\varepsilon \sigma_y d\varepsilon - \int_0^{\varepsilon_y} E\varepsilon d\varepsilon + \int_{\varepsilon_{sh}}^\varepsilon E_{sh}\left(\varepsilon - \varepsilon_{sh}\right) d\varepsilon\right\} dV_{sh} \end{aligned} \tag{3}$$

where ε is the normal strain at any fiber within a cross section, σ is the normal stress at any fiber within a cross section, E is the elastic modulus for the material, E_{sh} is the strain-hardening modulus of the material, V is the volume of fibers corresponding to their states within a cross section of an element, and subscripts e, $p(y)$, sh stand for elastic, plastic, and strain-hardening states of fiber elements, respectively. Fig. 3 illustrates cross-section partitions with fiber states, in which d_{CGe} and d_{CGsh} are the shift of the center of the initial neutral axis and the distance from the initial neutral axis to the strain-hardening neutral axis created by fibers in the strain-hardening regime, respectively.

Replacing the integrations over the volume of the element in Eq. (3) by integrating along the length and throughout the cross section of the element, Eq. (3) is expressed as

$$\begin{aligned} U = &\frac{E}{2}\int_L\int_{A_e} \varepsilon^2 dA_e dx + \sigma_y \int_L \int_{A_p} \varepsilon dA_p dx - \frac{1}{2}\sigma_y \varepsilon_y \int_L \int_{A_p} dA_p dx \\ &+ \frac{E_{sh}}{2}\int_L\int_{A_{sh}} \varepsilon^2 dA_{sh} dx + \left(\sigma_y - E_{sh}\varepsilon_{sh}\right)\int_L\int_{A_{sh}} \varepsilon dA_{sh} dx + \frac{1}{2}\left(E_{sh}\varepsilon_{sh}^2 - \sigma_y\varepsilon_y\right)\int_L\int_{A_{sh}} dA_{sh} dx \end{aligned} \tag{4}$$

where A_e is the remaining elastic area, A_p is the yielding area, A_{sh} is the strain-hardening area within a cross section, and L is the length of the element.

The normal strain of the assuming beam-column element can be predicted by the following strain-displacement relationship (Goto and Chen 1987)

$$\varepsilon = \frac{du}{dx} - y\frac{d^2v}{dx^2} + \frac{1}{2}\left(\frac{dv}{dx}\right)^2 \tag{5}$$

where u is a function describing the longitudinal displacements along the element, v is a function describing the transverse displacements, and dx is an infinitesimal length of element. In this formulation, linear shape functions and cubic Hermite shape functions are employed for longitudinal displacements and transverse displacements, respectively.

Substituting Eq. (5) into Eq. (4), the total internal strain energy of the partially strain-hardening elastic-plastic beam-column element is written as

$$\begin{aligned}
U = {} & \frac{E}{2}\int_0^L \left\{ A_e\left(\frac{du}{dx}\right)^2 - 2S_{ze}\left(\frac{d^2v}{dx^2}\right)\left(\frac{du}{dx}\right) + I_{ze}\left(\frac{d^2v}{dx^2}\right)^2 \right\} dx \\
& + \frac{E}{2}\int_0^L \left\{ A_e\left(\frac{du}{dx}\right)\left(\frac{dv}{dx}\right)^2 - S_{ze}\left(\frac{d^2v}{dx^2}\right)\left(\frac{dv}{dx}\right)^2 + \frac{A_e}{4}\left(\frac{dv}{dx}\right)^4 \right\} dx \\
& + \int_0^L \left\{ P_{A_p}\left(\frac{du}{dx}\right) - M_{A_p}\left(\frac{d^2v}{dx^2}\right) + \frac{P_{A_p}}{2}\left(\frac{dv}{dx}\right)^2 \right\} dx - \frac{1}{2}P_{A_p}\varepsilon_y\int_0^L dx \\
& + \frac{E_{sh}}{2}\int_0^L \left\{ A_{sh}\left(\frac{du}{dx}\right)^2 - 2S_{zsh}\left(\frac{d^2v}{dx^2}\right)\left(\frac{du}{dx}\right) + I_{zsh}\left(\frac{d^2v}{dx^2}\right)^2 \right\} dx \\
& + \frac{E_{sh}}{2}\int_0^L \left\{ A_{sh}\left(\frac{du}{dx}\right)\left(\frac{dv}{dx}\right)^2 - S_{zsh}\left(\frac{d^2v}{dx^2}\right)\left(\frac{dv}{dx}\right)^2 + \frac{A_{sh}}{4}\left(\frac{dv}{dx}\right)^4 \right\} dx \\
& + \left(\sigma_y - E_{sh}\varepsilon_{sh}\right)A_{sh}\int_0^L \left\{ \left(\frac{du}{dx}\right) + \frac{1}{2}\left(\frac{dv}{dx}\right)^2 \right\} dx \\
& - \left(\sigma_y - E_{sh}\varepsilon_{sh}\right)S_{zsh}\int_0^L \left(\frac{d^2v}{dx^2}\right) dx + \frac{1}{2}\left(E_{sh}\varepsilon_{sh}^2 - \sigma_y\varepsilon_y\right)A_{sh}\int_0^L dx
\end{aligned} \tag{6}$$

where characteristics of the cross section illustrated in Fig. 3 as follows

$$A_e = \sum_{j=1}^{o}\left(A_j\right)_e \qquad S_{ze} = d_{CGe}A_e \qquad I_{ze} = \sum_{j=1}^{o}\left(y_j^2A_j + I_{z,j}\right)_e \tag{7}$$

$$A_p = \sum_{j=1}^{p}\left(A_j\right)_p \qquad P_{A_p} = \sum_{j=1}^{p}\left(\sigma_{y,j}A_j\right)_p \qquad M_{A_p} = \sum_{j=1}^{p}\left(y_j\sigma_{y,j}A_j\right)_p \tag{8}$$

$$A_{sh} = \sum_{j=1}^{q}\left(A_j\right)_{sh} \qquad S_{zsh} = d_{CGsh}A_{sh} \qquad I_{zsh} = \sum_{j=1}^{q}\left(y_j^2A_j + I_{z,j}\right)_{sh} \tag{9}$$

where *o*, *p*, and *q* are the number of elastic, yielding, and strain-hardening fibers, respectively. $I_{z,j}$ is the *z*-axis moment of inertia of j^{th} fiber around its centroid, P_{A_p} and M_{A_p} are the resisting force and moment created by yielding fibers, respectively, and d_{CGe} and d_{CGsh} are the shift of the center of the initial neutral axis and the distance from the initial neutral axis to the new strain-hardening neutral axis created by fibers in the strain-hardening state, respectively.

The potential energy of the element with loads indicated in Fig. 1 can be expressed as

$$V = -\int_0^L w(x)v(x)dx - Pv(P) - \{r\}^T \{d\} \tag{10}$$

where $w(x)$ is a function of the distributed load, P is the magnitude of the concentrated load, $v(P)$ is the displacement at the position put by the concentrated load, $\{r\}$ is the nodal load vector applied at two ends of the element, and $\{d\}$ is the nodal displacement vector at the two ends of the element.

The total potential energy of the element is written as follows

$$\Pi = U + V \tag{11}$$

Applying the principle of stationary potential energy, the change in the total potential energy for element vanishes for small variations in the generalized coordinates at an equilibrium configuration. In mathematical terms, this can be written as: $\frac{\partial \Pi}{\partial d_i} = 0$ with i = 1, 2,..., 6. Taking the partial derivatives of Eq. (11), the set of equilibrium equations of the beam-column element can be given by

$$\{r\} = [K_{Se}]\{d\} + \{EF\} + \{r_p\} + \{r_{sh}\} \tag{12}$$

where $[K_{S_e}]$ is the element secant stiffness matrix, $\{r\}$ is the vector of element nodal forces, $\{EF\}$ is the vector of fixed end-forces due to the superposition of both distributed and concentrated loads, $\{r_p\}$ is the nodal load vector resisted by the yielding area of the cross section, and $\{r_{sh}\}$ is the nodal load vector resisted by the strain-hardening area of the cross section.

The element tangent stiffness matrix can be obtained by applying a truncated Taylor series expansion of the element equilibrium equations as follows

$$(r_i)_{new} - (r_i)_{old} = \frac{\partial r_i}{\partial d_j}\left[(d_j)_{new} - (d_j)_{old}\right] \tag{13}$$

$$K_{T(i,j)} = \frac{\partial r_i}{\partial d_j} = \frac{\partial^2 \Pi}{\partial d_j \partial d_i} \qquad \text{with} \qquad i, j = 1, 2, ..., 6 \tag{14}$$

$$[K_T] = [K_0] + [K_1] + [K_2] + [K_p] + [K_{sh0}] + [K_{sh1}] + [K_{sh2}] + [K_{psh}] \tag{15}$$

where $[K_0]$ is a linear stiffness matrix for elastic fibers, $[K_1]$ and $[K_2]$ are nonlinear geometric stiffness matrices for elastic fibers, $[K_p]$ is a plastic stiffness matrix for yielding fibers, $[K_{sh0}]$ is a linear stiffness matrix for strain-hardening fibers, $[K_{sh1}]$ and $[K_{sh2}]$ are nonlinear geometric stiffness

matrices for strain-hardening fibers, and [K_{psh}] is a plastic stiffness matrix for strain-hardening fibers. The details of these component matrices are presented in the appendix of Nguyen *et al*.'s study (Nguyen *et al*. 2014).

2.2 The effects of semi-rigid connections

2.2.1 Modified tangent stiffness matrix including semi-rigid connections

Semi-rigid connections are simulated by zero-length rotational springs attached at the two ends of the beam-column member developed above as illustrated in Fig. 5. Axial and shear deformations in connections are neglected. The static condensation algorithm (Wilson 1974) is again used to modify the beam-column member with eight degrees of freedom into the member with the conventional six degrees of freedom considering semi-rigid connections as shown in Fig. 6, and this also takes advantage of assembling the structural stiffness matrix. A similar procedure can be found in (Chen and Lui 1987). A modified process is presented as follows

Equilibrium equations of rotational spring elements at two beam ends are given by

$$\begin{bmatrix} R_{k1} & -R_{k1} \\ -R_{k1} & R_{k1} \end{bmatrix} \begin{Bmatrix} d_3 \\ d_7 \end{Bmatrix} = \begin{Bmatrix} r_3 \\ r_7 \end{Bmatrix} \tag{16}$$

$$\begin{bmatrix} R_{k2} & -R_{k2} \\ -R_{k2} & R_{k2} \end{bmatrix} \begin{Bmatrix} d_6 \\ d_8 \end{Bmatrix} = \begin{Bmatrix} r_6 \\ r_8 \end{Bmatrix} \tag{17}$$

where R_{k1} and R_{k2} are stiffness of rotational springs, and they are defined by the moment-rotation relationship of connections.

Equilibrium equations for the beam-column member, including nonlinear connections, with eight degrees of freedom are written as

$$\begin{bmatrix} (k_{33}+R_{k1}) & k_{36} & k_{13} & k_{23} & -R_{k1} & k_{34} & k_{35} & 0 \\ k_{36} & (k_{66}+R_{k2}) & k_{16} & k_{26} & 0 & k_{46} & k_{56} & -R_{k2} \\ k_{13} & k_{16} & k_{11} & k_{12} & 0 & k_{14} & k_{15} & 0 \\ k_{23} & k_{26} & k_{12} & k_{22} & 0 & k_{24} & k_{25} & 0 \\ -R_{k1} & 0 & 0 & 0 & R_{k1} & 0 & 0 & 0 \\ k_{34} & k_{46} & k_{14} & k_{24} & 0 & k_{44} & k_{45} & 0 \\ k_{35} & k_{56} & k_{15} & k_{25} & 0 & k_{45} & k_{55} & 0 \\ 0 & -R_{k2} & 0 & 0 & 0 & 0 & 0 & R_{k2} \end{bmatrix} \begin{Bmatrix} d_3 \\ d_6 \\ d_1 \\ d_2 \\ d_7 \\ d_4 \\ d_5 \\ d_8 \end{Bmatrix} = \begin{Bmatrix} r_3 \\ r_6 \\ r_1 \\ r_2 \\ r_7 \\ r_4 \\ r_5 \\ r_8 \end{Bmatrix} \tag{18}$$

$$\begin{bmatrix} K_{aa} & K_{ab} \\ K_{ba} & K_{bb} \end{bmatrix} \begin{Bmatrix} d_a \\ d_b \end{Bmatrix} = \begin{Bmatrix} r_a \\ r_b \end{Bmatrix} \tag{19}$$

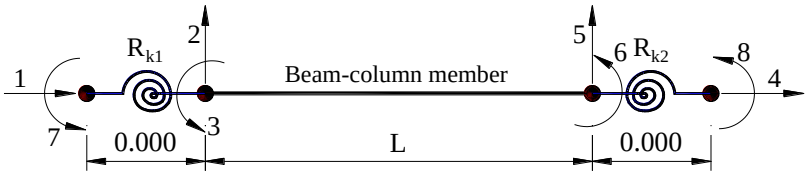

Fig. 5 Beam-column member including nonlinear connections with eight degrees of freedom

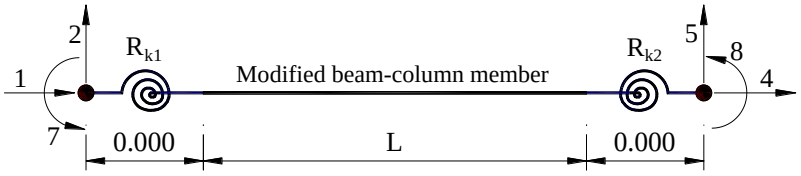

Fig. 6 Modified beam-column member with conventional six degrees of freedom

where d_a is the condensed displacement vector including two degrees of freedom and d_b is the displacement vector of the modified beam-column member with the conventional six degrees of freedom.

Rewriting Eq. (19) as algebraic equations

$$[K_{aa}]\{d_a\}+[K_{ab}]\{d_b\}=\{r_a\} \tag{20}$$

$$[K_{ba}]\{d_a\}+[K_{bb}]\{d_b\}=\{r_b\} \tag{21}$$

From Eq. (20), we have

$$\{d_a\}=[K_{aa}]^{-1}\{r_a\}-[K_{aa}]^{-1}[K_{ab}]\{d_b\} \tag{22}$$

Eq. (22) is used to solve the condensed displacements. Substituting Eq. (22) into Eq. (21), equilibrium equations including the essential six degrees of freedom are written as

$$\left([K_{bb}]-[K_{ab}]^T[K_{aa}]^{-1}[K_{ab}]\right)\{d_b\}=\{r_b\}-[K_{ab}]^T[K_{aa}]^{-1}\{r_a\} \tag{23}$$

$$[K']\{d_b\}=\{r'\} \tag{24}$$

From Eq. (23), we obtain the modified tangent stiffness matrix [K'] including nonlinear connections and the modified load vector {r'}.

2.2.2 Nonlinear moment-rotation relationship of semi-rigid connections

In this study, nonlinear behavior of semi-rigid connections is represented by a nonlinear moment-rotation curve. It is expressed by a mathematical function in which the parameters are determined by a fitted curve with test results. The Kishi-Chen model (Chen and Kishi 1989) and the Chen-Lui exponential model (Lui and Chen 1986) are employed for tracing nonlinear moment-

rotation behavior of semi-rigid connections. For more information about the modelling of semi-rigid connection behavior, readers can refer the review article (Díaz *et al*. 2011).

The Kishi-Chen model (Chen and Kishi 1989) is currently one of the most popular models used for semi-rigid connections since it needs only three parameters to capture the moment-rotation curve and always generates a positive stiffness. The moment-rotation relationship of the connection is presented by Chen and Kishi as follows

$$M = \frac{R_{ki}\left|\theta_r\right|}{\left[1+\left(\left|\theta_r\right|/\theta_0\right)^n\right]^{1/n}} \tag{25}$$

where M and θ_r are the moment and the rotation of the connection, n is the shape parameter, θ_0 is the reference plastic rotation, and R_{ki} is the initial connection stiffness.

Lui and Chen proposed the following exponential model (Lui and Chen 1986)

$$M = M_0 + \sum_{j=1}^{n} C_j\left(1-\exp^{-\frac{|\theta_r|}{2j\alpha}}\right) + R_{kf}\left|\theta_r\right| \tag{26}$$

where M and $|\theta_r|$ are the moment and the absolute value of the rotational deformation of the connection, respectively, α is the scaling factor, R_{kf} is the strain-hardening stiffness of the connection, M_0 is the initial moment, C_j is the curve-fitting coefficient, and n is the number of terms considered.

3. Nonlinear solution algorithm

In this section, a new numerical algorithm for solving the nonlinear structural equilibrium equation is proposed. The conventional Newton-Raphson algorithm combined with the constant work method for adjusting the incremental load factor is developed herein to solve the incremental equilibrium equation because of its simplicity and accuracy. The incremental form of the equilibrium equation can be written for the j^{th} iteration of the i^{th} incremental step as

$$\left[K_{T,j}^{i}\right]\left\{\Delta D_j^i\right\} = \left\{\Delta F_j^i\right\} \tag{27}$$

where $[K_{T,j}^{i}]$ is the tangent stiffness matrix, $\{\Delta D_j^i\}$ is the incremental displacement vector, and $\{\Delta F_j^i\}$ is the incremental load vector at the i^{th} incremental step (i.e., $j = 0$) or the unbalanced force vector for the subsequent iteration (i.e., $j \geq 1$).

The incremental element nodal displacement vector is calculated by extracting corresponding displacement degrees of freedom and transforming to the element local axis as

$$\left\{\Delta d_{e,j}^{i}\right\} = \left[L\right]\left\{\Delta \bar{d}_{e,j}^{i}\right\} \tag{28}$$

where $\{\Delta d_{e,j}^{i}\}$ is the element nodal displacement vector in the element local coordinate axis, $[L]$ is the global to local transformation matrix, and $\{\Delta \bar{d}_{e,j}^{i}\}$ is the displacement vector at two ends of an element in the global coordinate axis.

The incremental element forces are determined by the tangent element stiffness equation as

$$\left\{\Delta r_{e,j}^{i}\right\}=\left[k_{te,j}^{i}\right]\left\{\Delta d_{e,j}^{i}\right\} \tag{29}$$

Transforming the incremental element forces from the local axis to the global coordinate axis, the incremental element force vector in the element global coordinate axis are then calculated as

$$\left\{\Delta \bar{r}_{e,j}^{i}\right\}=[T]\left\{\Delta r_{e,j}^{i}\right\} \tag{30}$$

The resistance force vector of the whole structure can be assembled and computed as

$$\left\{R_{j}^{i}\right\}=\left\{R_{j-1}^{i}\right\}+\sum_{Nele}\left\{\Delta \bar{r}_{e,j}^{i}\right\} \tag{31}$$

Comparing the element forces against the applied load, the following equilibrium equation for unbalanced forces, $\{\Delta F_{j}^{i}\}$, is generated

$$\left[K_{T,j}^{i}\right]\left\{\delta D_{j+1}^{i}\right\}=\left\{\Delta F_{j}^{i}\right\}=\lambda^{i}\left\{F\right\}-\left\{R_{j}^{i}\right\} \tag{32}$$

where $\{F\}$ is the reference load vector at the i^{th} incremental step and $\{R_{j}^{i}\}$ is the accumulated incremental element force vector for the subsequent iteration (i.e., $j \geq 1$, $\{R_{j}^{i}\}=0$ for $j = 0$). λ^{i} is the incremental load factor at the i^{th} incremental step.

Once the incremental displacement vector $\{\delta D_{j+1}^{i}\}$ at the subsequent $(j + 1)_{\text{th}}$ iteration is determined, the accumulated incremental displacement vector $\{\Delta D_{j+1}^{i}\}$ and the total displacement vector $\{D_{j+1}^{i}\}$ of the structure at the i^{th} incremental step can be accumulated and updated as follows

$$\left\{\Delta D_{j+1}^{i}\right\}=\left\{\Delta D_{j}^{i}\right\}+\left\{\delta D_{j+1}^{i}\right\} \tag{33}$$

$$\left\{D_{j+1}^{i}\right\}=\left\{D_{j}^{i}\right\}+\left\{\delta D_{j+1}^{i}\right\} \tag{34}$$

The process is repeated until the equilibrium error is sufficiently small. A convergence check must be satisfied the following condition

$$\frac{\left\{\delta D_{j+1}^{i}\right\}^{T}\left\{\delta D_{j+1}^{i}\right\}}{\left\{\Delta D_{j+1}^{i}\right\}^{T}\left\{\Delta D_{j+1}^{i}\right\}} \leq Tolerance \tag{35}$$

The constant work method is adopted for estimating the incremental load factor for the next $(i + 1)^{\text{th}}$ incremental step by the following equations

$$\lambda^{i+1}=\sqrt{\frac{\delta w}{W_{j+1}^{i}}} \tag{36}$$

$$\delta w = \left(\lambda^1\right)^2 . W_0^1 \tag{37}$$

$$W_0^1 = \left\{\Delta D_0^1\right\} . \lambda^1 \left\{F\right\}^T \tag{38}$$

in which δw is the incremental reference work and λ^1 is the initial incremental load factor. W_{j+1}^i is the internal work for the i^{th} incremental step, defined as follows

$$W_{j+1}^i = \left\{\Delta D_{j+1}^i\right\}\left\{R_{j+1}^i\right\}^T \tag{39}$$

The details of procedure for the application of the proposed nonlinear solution algorithm are as follows:

Step 1. Select the initial incremental load factor λ^1 and calculate the incremental reference work δw using Eq. (36).

Step 2. Initialize $\{D_0^i\} = \{0\}$, $\{R_0^i\} = \{0\}$, $\{\Delta F_0^i\} = \lambda^1\{F\}$, etc.

Step 3. For the first iteration ($j = 0$) at each increment step i:

(a) Form the incremental load vector $\lambda^i \{F\}$.
(b) Form the global stiffness matrix $[K_{T,0}^i]$.
(c) Solve Eq. (27) for $\{\Delta D_0^i\}$.

Step 4. For the next iterations ($j \geq 1$):

(a) Calculate the unbalanced force using $\{\Delta F_j^i\} = \lambda^i\{F\} - \{R_j^i\}$.
(b) Update the global stiffness matrix $[K_{T,j}^i]$.
(c) Solve Eq. (32) for $\{\delta D_{j+1}^i\}$.

Step 5. Check the termination: If the determination of the tangent stiffness matrix of the structure is smaller than or equal to zero, stop the procedure. Otherwise, go to Step 6.

Step 6. Calculate the displacements at two ends of members and the displacements along the member length.

Step 7. Calculate stresses of fibers using Eq. (2). Update the characteristics of the cross section using Eqs. (7), (8), and (9). Define the tangent stiffness of connections using $R_{kt} = \dfrac{dM}{d\,|\,\theta_r\,|}$.

Step 8. Update the accumulated incremental displacement $\{\Delta D_{j+1}^i\}$ using Eq. (33) and update the total displacement $\{D_{j+1}^i\}$ of the structure using Eq. (34).

Step 9. Calculate the resistance force $\{R_j^i\}$ using Eq. (31)

Step 10. Check the convergence: if the ratio of the norm of the incremental displacement $\{\delta D_{j+1}^i\}$ to the norm of the accumulated incremental displacement $\{\Delta D_{j+1}^i\}$ is smaller than the preset tolerance as Eq. (35), go to Step 11. Otherwise, let $j = j + 1$ and return to Step 4.

Step 11. Check the termination: if the total number of steps is smaller than the preset number N, determine the incremental load factor λ^{i+1} using Eq. (36), then let $i = i + 1$ and go to Step 3. Otherwise, stop the procedure.

A simplified flow chart of the proposed analysis procedure is illustrated in Fig. 7.

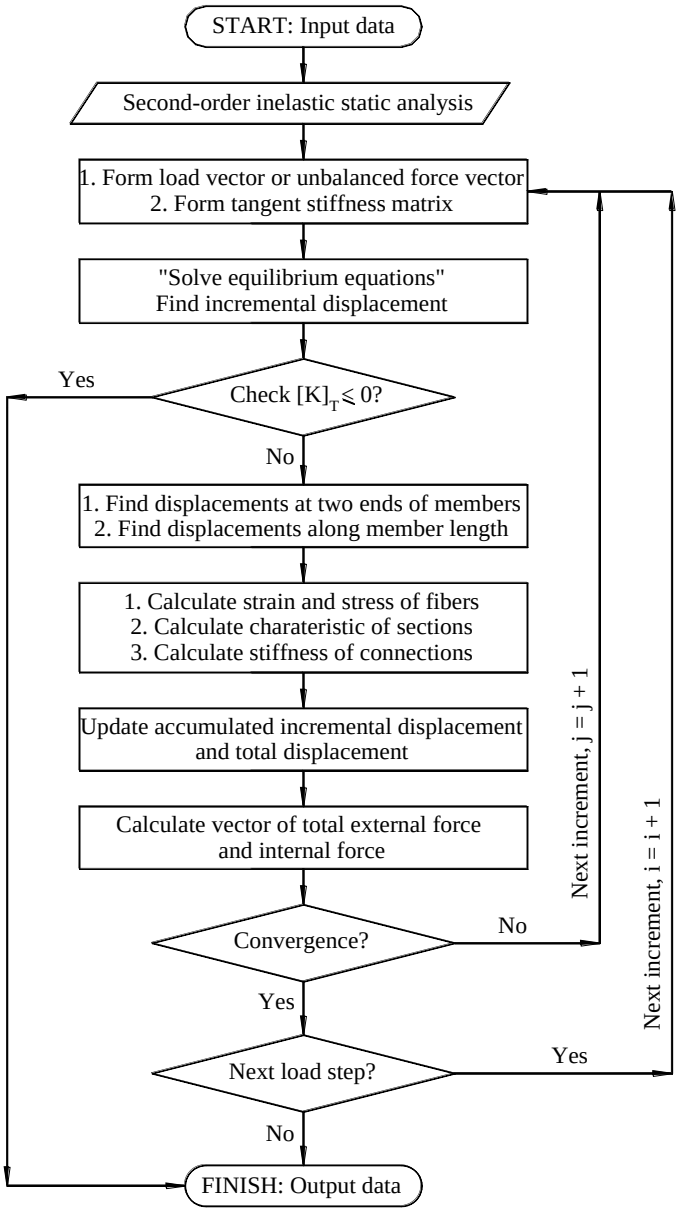

Fig. 7 Simplified analysis flowchart

4. Numerical examples and discussions

A computer program written in the C^{++} programming language is developed based on the above mentioned formulations and procedures to predict second-order distributed plasticity static behavior of plane steel frames with nonlinear semi-rigid beam-to-column connections. It is verified for accuracy and reliability by the comparison of the predictions with those obtained by previous studies in the literature. The initial ECCS residual stress (ECCS 1984) shown in Fig. 8 is

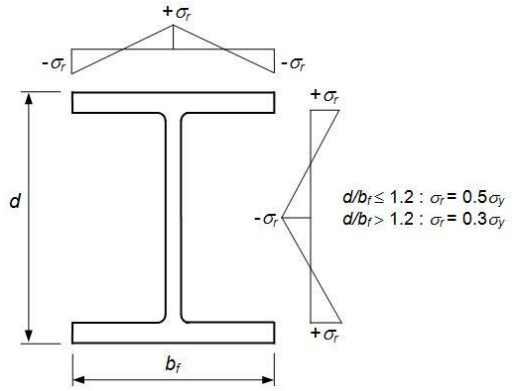

Fig. 8 The ECCS residual stress pattern for I-section

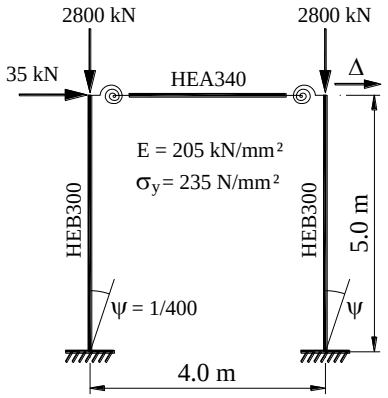

Fig. 9 Vogel portal steel frame with semi-rigid connections

assumed to be distributed uniformly along the member length. All the frame members are divided into 40 discrete elements. Each cross-section of elements is divided into 66 fibers (27 at each flange, 12 at the web) as shown in Fig. 3.

4.1. Vogel portal steel frame

Vogel (1985) investigated the portal rigid steel frame using the distributed plasticity method as the European calibration frame for second-order inelastic analysis methods. The configuration of the frame with semi-rigid beam-to-column connections is shown in Fig. 9. The initial out-of-plumbness of ψ = 1 / 400 and the initial ECCS residual stress (ECCS 1984) are assumed for the frame. Young's modulus and the yield stress of steel are E = 20500 N/mm^2 and σ_y = 235 N/mm^2, respectively. For the distributed plasticity analysis, Vogel used 50 elements for the columns and 40 elements for the beam, and the proposed program used 40 elements for the columns and 40 elements for the beam. The cross section is discretized into 66 fibers (54 at both flanges, 12 at the web). The main aim of this analysis is to verify and perform the capability of the proposed program in capturing the second-order inelastic behavior accurately. For the frame with rigid connections, the obtained results using the proposed program are compared with those predicted by Vogel (1985) and Nguyen and Kim (2014) as illustrated in Fig. 10. It can be seen that the load-displacement curves of Nguyen and Kim with shear deformation and the proposed program are identical, while the load-displacement curve of Vogel without shear deformation is higher. Percentage of section-areas in yielding at the ultimate load of the rigid frame is compared in Fig. 11(a). The proposed analysis generates values of percentage of yielding lower than the Vogel result. The ultimate load of 1.001 generated by the proposed program is lower that of 1.022 obtained by Vogel as compared in Table 1.

The rigid beam-to-column connections are replaced by semi-rigid ones to study the second-order inelastic behavior including the connection nonlinearity by Chen and Kim (1997) using the plastic hinge method. The three parameters for the Kishi-Chen power model of these semi-rigid connections are: R_{ki} = 31,635 kN·m/rad, M_u = 142 kN·m, and n = 0.98. The results of the proposed program and Nguyen and Kim (2014) in predicting the second-order inelastic response of the semi-rigid frame shown in Fig. 10. It can be seen that the nonlinear load – displacement curves agree well. The ultimate load factor obtained from the proposed analysis is 0.922 lower than

Table 1 Comparison of ultimate load factor of Vogel portal frame with various beam-to-column connections

Frame type	Method	Ultimate load factor	Difference (%)
Rigid	Distributed plasticity (Vogel 1985) (50ele column, 40ele beam)	1.022	–
	Fiber beam-column (Nguyen and Kim 2014), (2 integration points)	1.009	-1.27
	Distributed plasticity – Proposed (40ele column, 40ele beam)	1.001	-2.05
Semi-rigid	Fiber beam-column (Nguyen and Kim 2014), (2 integration points)	0.940	–
	Distributed plasticity – Proposed (40ele column, 40ele beam)	0.922	-1.91
Pinned	Fiber beam-column (Nguyen and Kim 2014), (2 integration points)	0.772	–
	Distributed plasticity – Proposed (40ele column, 40ele beam)	0.718	-6.99

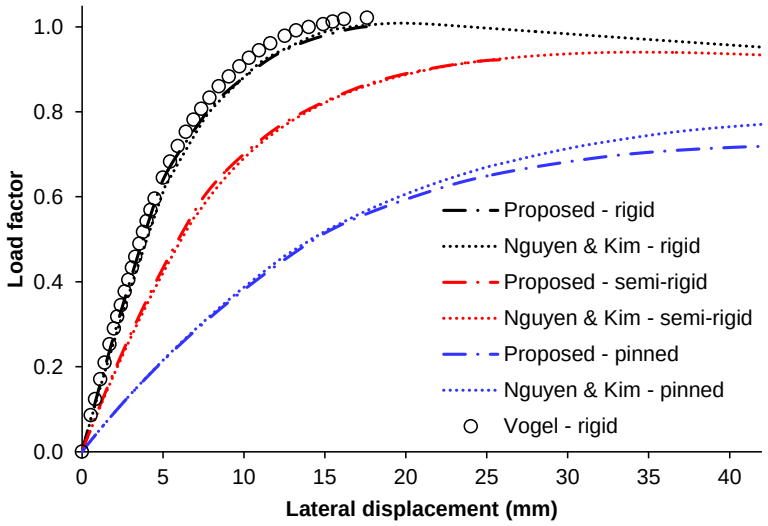

Fig. 10 Load – displacement curves of Vogel portal frame with various beam-to-column connections

1.91% of 0.940 produced by Nguyen and Kim. The load – displacement curve and the ultimate load factor of the frame with pinned beam-to-column connections is also shown and compared in Fig. 10 and Table 1. Percentage of section-areas in yielding at the ultimate load of the frame with pinned and semi-rigid connections is illustrated in Figs. 11(b)-(c), respectively. It can be seen that percentage of section-areas in yielding at top of two columns reduces clearly when rigidity of beam-to-column connections changes from fully rigid to ideally pinned.

With the personal computer configuration of AMD Phenom II X4 955 Processor, 3.2 GHz, and

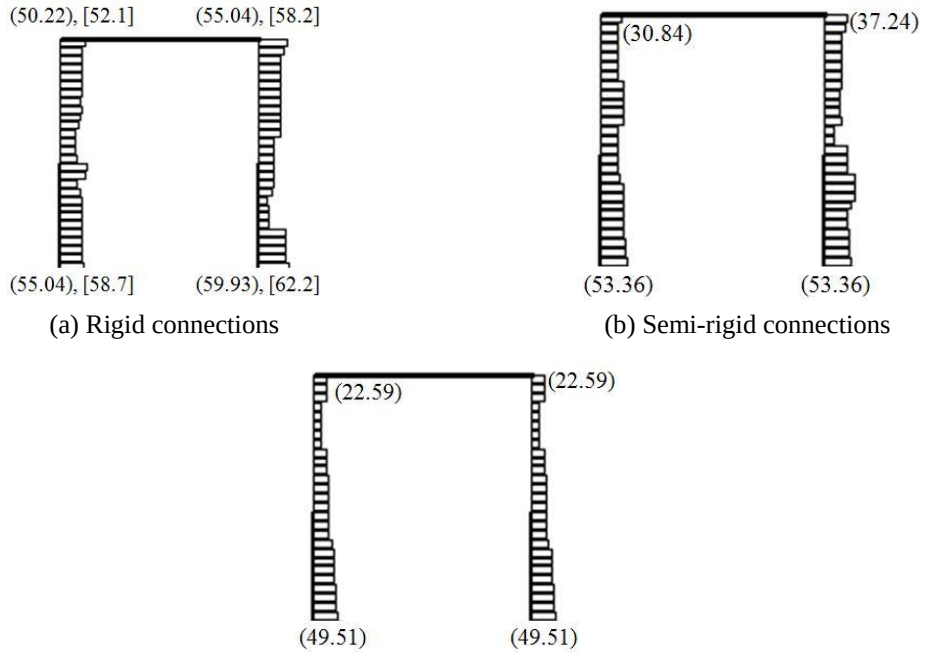

(a) Rigid connections (b) Semi-rigid connections

(c) Pinned connections

Fig. 11 Percentage of section-areas in yielding at ultimate load of Vogel portal frame with various beam-to-column connections ((--), [--] are values of the proposed program and Vogel, respectively)

8.00 GB RAM, the analysis time of the proposed program for the rigid, semi-rigid and pinned frames are 33, 56 and 35 s, respectively, using the initial incremental load step of 0.001. This result demonstrates the high computational efficiency of the proposed program.

4.2 Vogel two-bay six-story steel frame

Vogel two-bay six-story steel frame was also solved by Vogel (1985) as the European calibration frame for considering both the effects of geometric nonlinearities and distributed plasticity. The configuration and applied loads of the frame with semi-rigid beam-to-column connections is illustrated in Fig. 12. The geometric imperfections are considered by the initial out-of-plumbness of ψ = 1 / 450 for all column members and the initial ECCS residual stress (ECCS 1984) as shown in Fig. 8. Young's modulus and the yield stress of steel are E = 20500 N/mm^2 and σ_y = 235 N/mm^2, respectively. In this analysis, the proposed program uses 40 elements for both beam and column members. The cross sections of all elements are discretized into 66 fibers (54 at both flanges, 12 at the web). For the frame with rigid connections, the results of the load-displacement curve and the ultimate load factor are compared in Fig. 13 and Table 2, respectively. The ultimate load factor of 1.110 obtained by the proposed program is in agreement with Vogel's result using the same distributed plasticity method. The ultimate load factor generated by other researches also is listed in Table 2. It can be concluded that the proposed program accurately predicts the nonlinear behavior and strength of steel frames considering both the geometric nonlinearities and distributed plasticity.

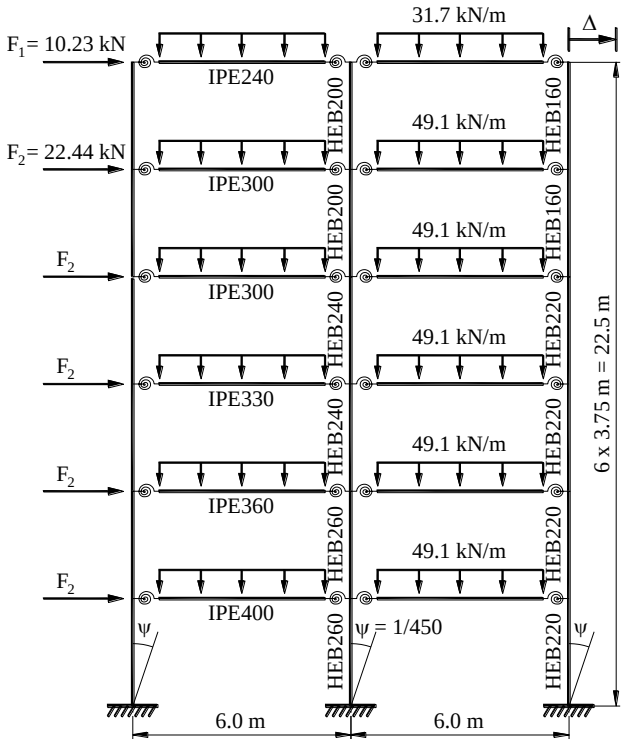

Fig. 12 Vogel two-bay six-story steel frame with semi-rigid connections

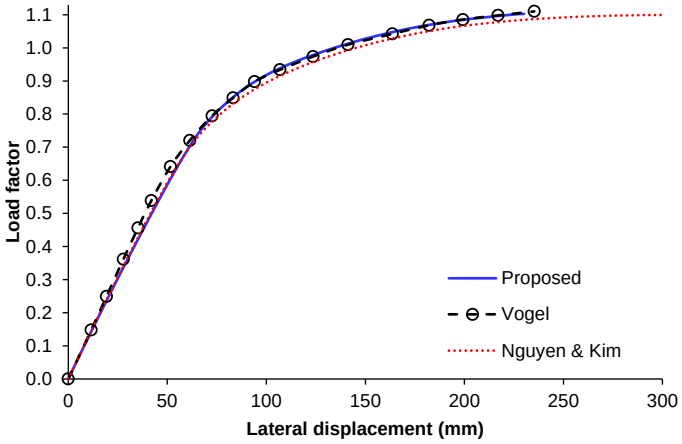

Fig. 13 Load – displacement curves of Vogel six-story frame with rigid connections

Chan and Chui (2000) built in the semi-rigid connections at beam ends to study a more realistic nonlinear behavior of the frame, as shown in Fig. 12. The curve fitted parameters of the Chen-Lui exponential model for both flush end plate (type C) and single web angle (type A) connections are listed in Table 3. Fig. 14 shows the nonlinear moment-rotation curves of these connections. The load-displacement curves of the proposed analysis are slightly different with those of Nguyen and

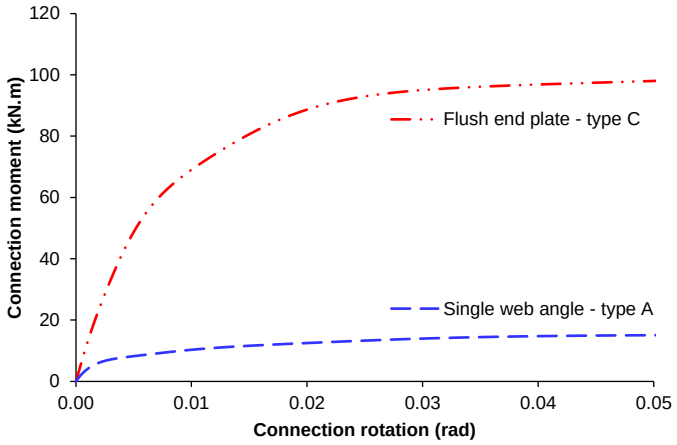

Fig. 14 Moment-rotation curves of semi-rigid connections for Vogel six-story frame

Table 2 Comparison of ultimate load factor of Vogel six-story frame with rigid connections

Method	Ultimate load factor	Difference (%)
Distributed plasticity (Vogel 1985)	1.110	–
Plastic hinge (Vogel 1985)	1.120	+0.90
Refined plastic hinge (Chan and Chui 2000)	1.125	+1.35
Fiber beam-column (Nguyen and Kim 2014)	1.100	-0.90
Distributed plasticity – Proposed	1.110	+0.00

Table 3 Parameters of connections for the Chen-Lui exponential model

	Semi-rigid connections	
	A - Single web angle	C - Flush end plate
Tested by	Richard *et al*. (1982)	Ostrander (1970)
M_0 (kN.m)	0.000	0.000
R_{kf} (kN·m/rad)	5.322	108.925
α	0.00051167	0.00031783
C1	-4.892	-28.287
C2	137.140	573.189
C3	-661.841	-3433.984
C4	1465.397	8511.301
C5	-1510.926	-9362.567
C6	590.000	3832.899
R_{ki} (kN·m/rad)	5440.592	12340.198

Kim (2014), as illustrated in Fig. 15. It can be seen that the load-displacement curves of the frame with various semi-rigid connections predicted by the proposed analysis are slightly lower than those of Nguyen and Kim (2014) using the fiber plastic beam-column method. This difference is due to the fact that the Nguyen and Kim's method applied equivalent concentrated loads for beams

Table 4 Comparison of ultimate load factor of Vogel six-story frame with various semi-rigid connections

Connection type	Method	Ultimate load factor	Difference (%)
Type C	Fiber beam-column (Nguyen and Kim 2014)	0.817	–
	Distributed plasticity – Proposed	0.777	-4.90
Type A	Fiber beam-column (Nguyen and Kim 2014)	0.297	–
	Distributed plasticity – Proposed	0.287	-3.37

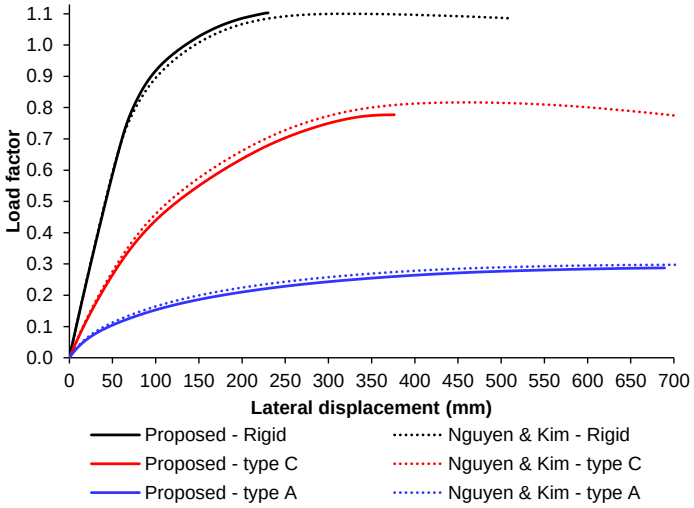

Fig. 15 Load – displacement curves of Vogel six-story frame with various beam-to-column connections

instead of simulating uniformly distributed loads; hence, distributed plasticity in the beam members using Nguyen and Kim's method is not accurate as the proposed method. The ultimate load factor of the frame with various semi-rigid connections obtained by the proposed program and Nguyen and Kim (2014) is compared in Table 4. Fig. 16 illustrates percentage of section-areas in yielding at the ultimate load of the frame with various beam-to-column connections.

4.3 Wong four-bay five-story steel frame – A case study

The layout of a four-bay five-story steel frame located in Shanghai, China, is investigated. Wong (1995) studied the static load-displacement analysis of a similar frame with flush end plate connections. The geometric configuration of the frame is shown in Fig. 17. The initial ECCS residual stress pattern (ECCS 1984) is assigned for all members as shown in Fig. 8 In this study, the frame with the flush end plate and rigid connection types are considered for comparison. The flush end plate connection tested by Ostrander (1970) was represented by the Chen-Lui exponential model (Lui and Chen 1986). The parameters and moment-rotation curve of the model for the flush end plate connection are shown in Table 3 and Fig. 14, respectively. 40 elements per column and beam members are employed in modeling of the frame. The ultimate load factors of the frame with the rigid and semi-rigid connections are 1.381 and 0.659, respectively. The load-displacement curves are plotted in Fig. 18. Fig. 19 illustrates percentage of section-areas in

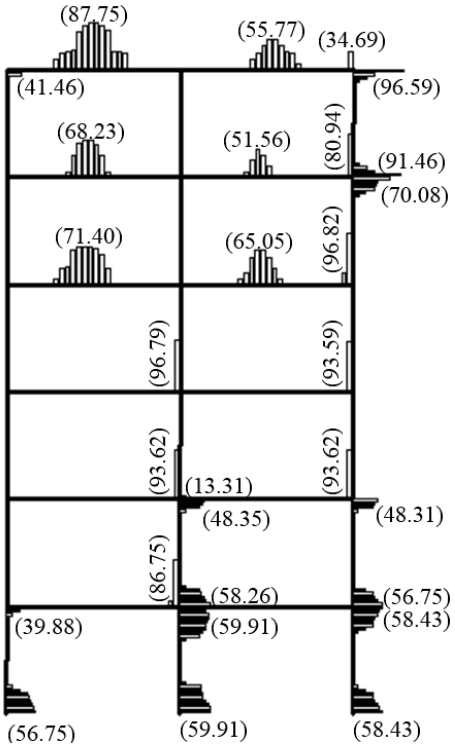

(a) Rigid connections

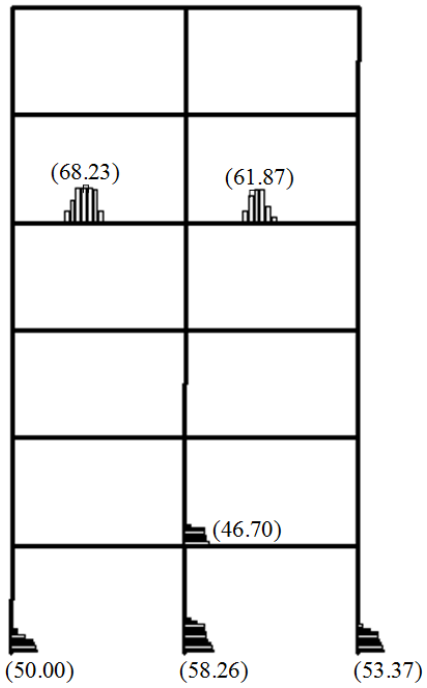

(b) Type-C connections

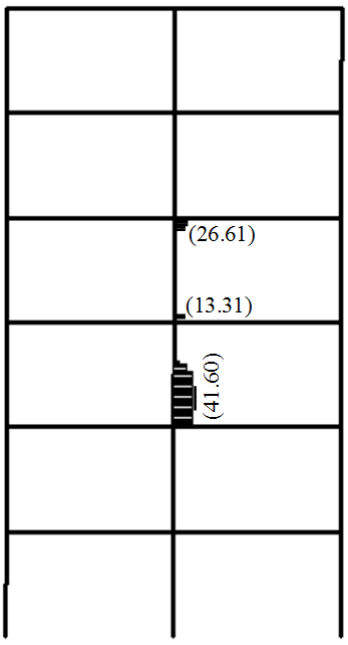

(c) Type-A connections

Fig. 16 Percentage of section-areas in yielding at ultimate load of Vogel six-story frame with various beam-to-column connections

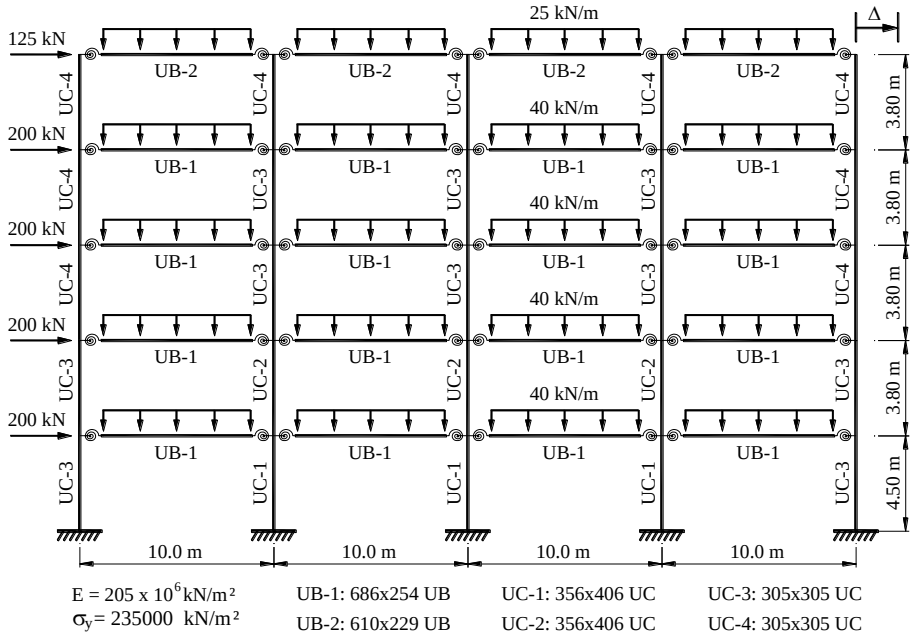

Fig. 17 Wong four-bay five-story steel frame with semi-rigid connections

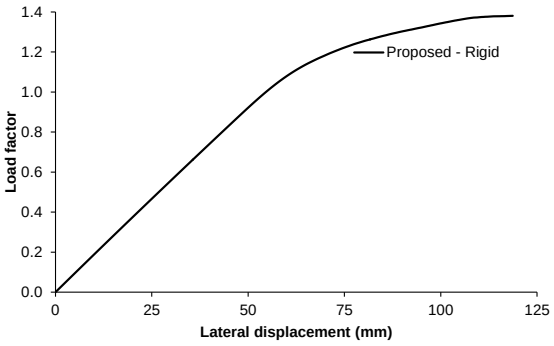

(a) Rigid connections

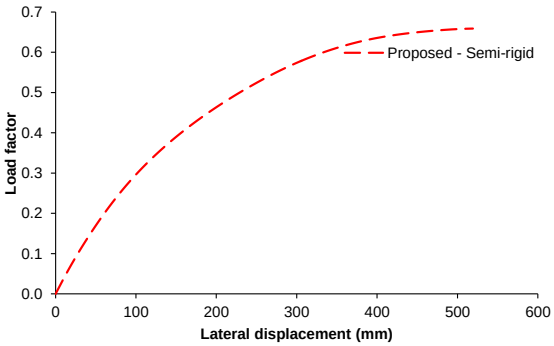

(b) Type-C connections

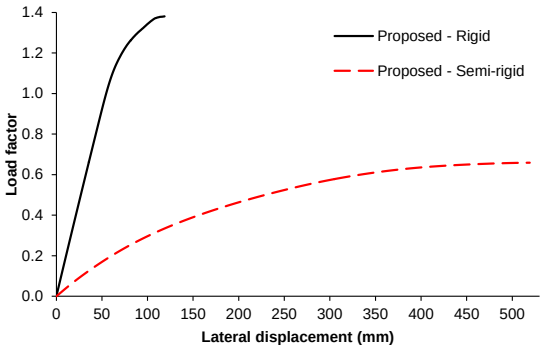

(c) Comparing between (a) and (b)

Fig. 18 Load – displacement curves of Wong frame with various beam-to-column connections

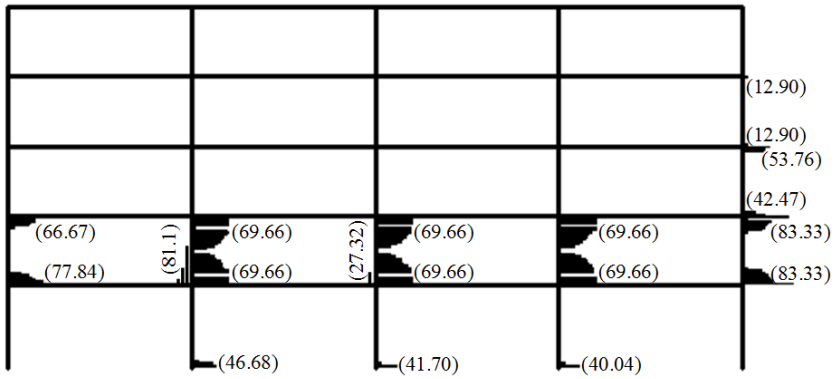

(a) Rigid connections

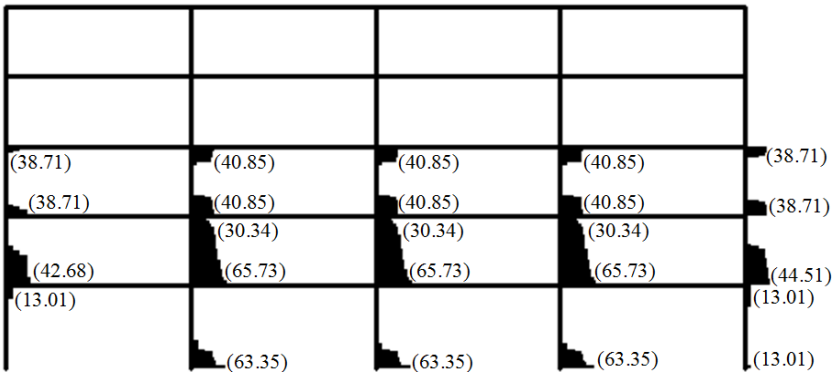

(b) Semi-rigid connections

Fig. 19 Percentage of section-areas in yielding at ultimate load of Wong frame with various beam-to-column connections

yielding at the ultimate load of the frame with various beam-to-column connections. It can be concluded that the main reason for collapsing of both frame types is due to yielding along the three middle columns of the second floor. With the rigid frame, yielding initially forms at both the bottom and the top of the three middle columns of the second floor and gradually spreads into the middle of the columns, whereas with the semi-rigid frame, yielding initially forms at the bottom of the three middle columns of the second floor and gradually spreads up to the top of the columns. It can be concluded that semi-rigid connections play an important role in the static response of steel framed structures.

5. Conclusions

An accurate numerical procedure is presented for the second-order distributed plasticity analysis of planar steel frames under static loadings. By assuming that steel behaves as an elastic-perfectly plastic material with linear strain hardening, a new nonlinear beam-column stiffness matrix including flexibility of nonlinear connections is proposed in this study. The effects of gradual yielding, geometric nonlinearity, connection flexibility, moving of the neutral axis, initial

member out-of-straightness, and residual stress can be directly taken into account through the element tangent stiffness matrix. The accuracy and efficiency of the proposed procedure are proved by comparing the results with previous studies. The following conclusions can be drawn from the present study:

- Percentage of yielding of the whole framed structure is performed. This helps for designing more accurately and completely.
- The flexibility of nonlinear semi-rigid connections plays an important role in the overall structural responses during the incremental iteration procedure of static loadings.
- It is necessary to include initial geometric imperfections and connection flexibility into advanced analysis methods to increase accuracy and safety for performance-based designs of steel frames.
- The presented numerical examples can be used to verify the validity and accuracy of another advanced analysis methods as benchmarks.
- The proposed program can be also used to develop three-dimensional advanced analysis programs for framed structures subjected to static and dynamic loadings.

Acknowledgments

This work was supported by the National Research Foundation (NRF) of Korea grant funded by the Korean government (MSIP) (No. 2011-0030040) and (No. 2015R1A2A2A01007339).

References

Alemdar, B.N. and White, D.W. (2005), "Displacement, flexibility, and mixed beam–column finite element formulations for distributed plasticity analysis", *J. Struct. Eng.*, **131**(12), 1811-1819.

Attalla, M.R., Deierlein, G.G. and McGuire, W. (1994), "Spread of plasticity: Quasi-plastic-hinge approach", *J. Struct. Eng.*, **120**(8), 2451-2473.

Avery, P. and Mahendran, M. (2000), "Distributed plasticity analysis of steel frame structures comprising non-compact sections", *Eng. Struct.*, **22**(8), 901-919.

Bandyopadhyay, M., Banik, A.K. and Datta, T.K. (2015), *Numerical Modeling of Compound Element for Static Inelastic Analysis of Steel Frames with Semi-rigid Connections*, Springer, India.

Chan, S.L. and Chui, P.P.T. (2000), *Nonlinear Static and Cyclic Analysis of Steel Frames with Semi-rigid Connections*, Elsevier, Amsterdam, The Netherlands.

Chen, W.F. and Kim, S.E. (1997), *LRFD Steel Design using Advanced Analysis*, CRC Press, Boca Raton, New York, NY, USA.

Chen, W.F. and Kishi, N. (1989), "Semirigid steel beam-to-column connections – Data-base and modeling", *J. Struct. Eng.-Asce*, **115**(1), 105-119.

Chen, W.F. and Lui, E.M. (1987), "Effects of joint flexibility on the behavior of steel frames", *Comput. Struct.*, **26**(5), 719-732.

Chiorean, C.G. (2009), "A computer method for nonlinear inelastic analysis of 3D semi-rigid steel frameworks", *Eng. Struct.*, **31**(12), 3016-3033.

Díaz, C., Martí, P., Victoria, M. and Querin, O.M. (2011), "Review on the modelling of joint behaviour in steel frames", *J. Construct. Steel Res.*, **67**(5), 741-758.

ECCS (1984), *Ultimate Limit State Calculation of Sway Frames with Rigid Joints*, European Convention for Constructional Steelwork, Technical Committee 8 – Structural Stability Technical Working Group 8.2.

Foley, C.M. (2001), "Advanced analysis of steel frames using parallel processing and vectorization", *Comput.-Aid. Civil Infrastruct. Eng.*, **16**(5), 305-325.

Foley, C.M. and Vinnakota, S. (1997), "Inelastic analysis of partially restrained unbraced steel frames", *Eng. Struct.*, **19**(11), 891-902.
Foley, C.M. and Vinnakota, S. (1999), "Inelastic behavior of multistory partially restrained steel frames. Part I", *J. Struct. Eng.-Asce*, **125**(8), 854-861.
Gorgun, H. (2013), "Geometrically nonlinear analysis of plane frames composed of flexibly connected members", *Struct. Eng. Mech., Int. J.*, **45**(3), 277-309.
Goto, Y. and Chen, W.F. (1987), "On the computer-based design analysis for the flexibly jointed frames", *J. Construct. Steel Res.*, **8**, 203-231.
Hoang, V.-L., Nguyen Dang, H., Jaspart, J.-P. and Demonceau, J.-F. (2015), "An overview of the plastic-hinge analysis of 3D steel frames", *Asia Pacific J. Computat. Eng.*, **2**(1), 1-34.
Kim, S.E. and Lee, D.H. (2002), "Second-order distributed plasticity analysis of space steel frames", *Eng. Struct.*, **24**(6), 735-744.
King, W.S., White, D.W. and Chen, W.F. (1992), "Second-order inelastic analysis methods for steel-frame design", *J. Struct. Eng.*, **118**(2), 408-428.
Lui, E.M. and Chen, W.F. (1986), "Analysis and behavior of flexibly-jointed frames", *Eng. Struct.*, **8**(2), 107-118.
Mahendran, M. and Avery, P. (2000), "Analytical benchmark solutions for steel frame structures subject to local buckling effects", *Adv. Struct. Eng.*, **3**(3), 215-229.
Nguyen, P.-C. and Kim, S.-E. (2014), "An advanced analysis method for three-dimensional steel frames with semi-rigid connections", *Finite Elem. Anal. Des.*, **80**, 23-32.
Nguyen, P.-C. and Kim, S.-E. (2015), "Second-order spread-of-plasticity approach for nonlinear time-history analysis of space semi-rigid steel frames", *Finite Elem. Anal. Des.*, **105**, 1-15.
Nguyen, P.-C., Doan, N.T.N., Ngo-Huu, C. and Kim, S.-E. (2014), "Nonlinear inelastic response history analysis of steel frame structures using plastic-zone method", *Thin-Wall. Struct.*, **85**, 220-233.
Ostrander, J.R. (1970), *An Experimental Investigation of End-plate Connections*, University of Saskatchewan, Saskatoon, Saskatchewan, Canada.
Richard, R.M., Kriegh, J.D. and Hormby, D.E. (1982), "Design of single plate framing connections with A307 bolts", *Eng. J.-Amer. Inst. Steel Constr.*, **19**(4), 209-213.
Rigobello, R., Coda, H.B. and Neto, J.M. (2013), "Inelastic analysis of steel frames with a solid-like finite element", *J. Construct. Steel Res.*, **86**, 140-152.
Saritas, A. and Koseoglu, A. (2015), "Distributed inelasticity planar frame element with localized semi-rigid connections for nonlinear analysis of steel structures", *Int. J. Mech. Sci.*, **96-97**, 216-231.
Teh, L.H. and Clarke, M.J. (1999), "Plastic-zone analysis of 3D steel frames using beam elements", *J. Struct. Eng.-Asce*, **125**(11), 1328-1337.
Toma, S. and Chen, W.-F. (1992), "European calibration frames for second-order inelastic analysis", *Eng. Struct.*, **14**(1), 7-14.
Valipour, H.R. and Bradford, M.A. (2013), "Nonlinear P-D analysis of steel frames with semi-rigid connections", *Steel Compos. Struct., Int. J.*, **14**(1), 1-20.
Vogel, U. (1985), "Calibrating frames", *Stahlbau, Berlin, Germany*, **54**(10), 295-301.
White, D.W. (1993), "Plastic-hinge methods for advanced analysis of steel frames", *J. Construct. Steel Res.*, **24**(2), 121-152.
White, D.W. and Chen, W.F. (1993), *Plastic Hinge based Methods for Advanced Analysis and Design of Steel Frames - An Assessment of the State of the Art*, Structural Stability Research Council, Lehigh University, Bethlehem, PA, USA.
Wilson, E.L. (1974), "The static condensation algorithm", *Int. J. Numer. Methods Eng.*, **8**(1), 198-203.
Wong, H.P. (1995), "A study on the behavior of realistic steel buildings using design and rigorous approaches", Master Thesis; Hong Kong Polytechnic University, Hong Kong.

CC